DR. FÁBIO A. ABADE DOS SANTOS (Orcid ID : 0000-0002-0696-7322)

DR. KEVIN P DALTON (Orcid ID : 0000-0002-7086-1979)

DR. FRANCISCO PARRA (Orcid ID : 0000-0002-1885-9521)

Article type   : Original Article

Title

Spillover events of Rabbit Hemorrhagic Disease Virus 2 (recombinant GI.4P-GI.2) from Lagomorpha to Eurasian badger

Authors:

Abade dos Santos, F.A.[1,2,3], DVM, MSc (fabio.abade@iniav.pt)

Pinto, A. [4], Lic, MSc

Burgoyne, [4,5,] Thomas BSc, PhD

Dalton, K.P. [3], BSc, PhD

Carvalho, C.L. [2], DVM, PhD

Ramilo, D.W. [1], DVM, MSc, PhD

Carneiro, C. [1], Grad, MSc

Carvalho, T. [6], DVM, PhD

Peleteiro, M.C.[1], DVM, MSc, PhD, ECVP

Parra, F. [3], BSc, PhD

Duarte, M.D.[1,2], DVM, MSc, PhD

Affiliations:

[1]Centre for Interdisciplinary Research in Animal Health (CIISA), Faculty of Veterinary Medicine, University of. Av. da Universidade Técnica, 1300-477 Lisbon, Portugal.

[2]INIAV IP- National Institute for Agrarian and Veterinary Research, Av. da República, Quinta do Marquês, 2780-157 Oeiras, Portugal.

[3]Instituto Universitario de Biotecnología de Asturias (IUBA), Departamento de Bioquímica y Biología Molecular, Universidad de Oviedo, Oviedo, Spain.

[4]Paediatric Respiratory Medicine, Primary Ciliary Dyskinesia Centre, Royal Brompton & Harefield NHS Trust, London, SW3 6NP, UK.

[5]UCL Institute of Ophthalmology, University College London, EC1V 9EL London, United Kingdom.

[6]Champalimaud Center for the Unknown, Champalimaud Foundation, Av. Brasilia, 1400-038 Lisboa, Portugal.

Corresponding Author

Fábio A. Abade dos Santos

e-mail: fabio.abade@iniav.pt

INIAV IP- National Institute for Agrarian and Veterinary Research, Av. da República, Quinta do Marquês, 2780-157 Oeiras, Portugal

Abstract

Rabbit haemorrhagic disease (RHD) is a major threat to domestic and wild European rabbits. Presently, in Europe, the disease is caused mainly by Rabbit haemorrhagic disease virus 2 (RHDV2/b or *Lagovirus europaeus* GI.2), the origin of which is still unclear, as no RHDV2 reservoir hosts were identified. After the RHDV2 emergence in 2010, viral RNA was detected in a few rodent species. Furthermore, RHDV2 was found to cause disease in some hare species resembling the disease in rabbits, evidencing the ability of the virus to cross the species barrier.

In this study, through molecular, histopathologic, antigenic and morphological evidences, we demonstrate the presence and replication of RHDV2 in Eurasian badgers (*Meles meles*) found dead in the district of Santarém, Portugal, between March 2017 and January 2020. In two of these seven animals, we further classify the RHDV2 as a *Lagovirus europaeus* recombinant GI.4P-GI.2.

Our results indicate that *Meles meles* is susceptible to RHDV2, developing systemic infection, and excreting the virus in the faeces. Given the high viral loads seen in several organs and matrices, we believe that transmission to the wild rabbit is likely.

Furthermore, transmission electron microscopy data shows the presence of Calicivirus compatible virions in the nucleus of hepatocytes, which has not been demonstrated before and constitutes a paradigm shift for caliciviruses's replication cycle.

1. Introduction

Rabbit haemorrhagic disease virus 2 (RHDV2, also referred to as *Lagovirus europaeus* GI.2 or RHDVb (Le Pendu et al., 2017), is a highly contagious Lagovirus of the Caliciviridae family that causes an acute infection in wild and domestic European rabbits (*Oryctolagus cuniculus*).

The virion measures from 27 to 40 nm (Ohlinger et al., 1990; Capucci et al., 1991) in diameter with the icosahedral typical morphology of the Caliciviridae, and a surface consisting of regularly arranged, cup-shaped depressions (Ohlinger et al., 1990; Capucci et al., 1991). The genomic material is composed of a single-stranded, non-segmented, positive-sense RNA genome of 7,437 nucleotides (Meyers et al., 1991). Also, the virus contain a sub-genomic 2.2 kb RNA, collinear to the 3' region of the genome (Ohlinger et al., 1990).

RHDV2 emerged in 2010 (Le Gall-Recule et al., 2011), and rapidly replaced the former circulating RHDV classical strains (GI.1) in several European countries, also expanding the disease to many regions in the world (Mahar et al., 2018). Since 2012, no RHDV GI.1 strains (former G1 to G6), have been reported in the Iberian Peninsula. Following the detection of RHDV2 strains, recombinant strains containing the non-structural region of GI.1 or non-pathogenic RHDV strains (GI.3 and GI.4) and the structural region of RHDV2 (GI.2) strains were identified. Several recombination breaking points have been described (Silvério et al., 2018). The recombinant hotspot located at the RdRp/VP60 level seems to play an important

role in the evolution of the new variants (Dalton et al., 2018; Silvério et al., 2018; Abrantes et al., 2020).

Other than the domestic and wild rabbit, RHDV2 has also been reported in several hare species, namely the Sardinian Cape hare (*Lepus capensis mediterraneus*) (Puggioni et al., 2013), the Italian hare (*Lepus corsicanus*) (Camarda et al., 2014), the European brown hare (*Lepus europaeus*) (Velarde et al., 2017) and the Mountain hare (*Lepus timidus*) (Neimanis et al., 2018) and recently in the jackrabbit (*Lepus californicus*), desert cottontails (*Sylvilagus audubonii*) and eastern cottontail (*Sylvilagus floridanus*) (USDA, 2020), causing haemorrhagic disease similar to that of the European rabbit.

This virus' ability to infect hares, alongside with the high fatality rates in both young and adult rabbits (Le Gall-Recule et al., 2011), contrast the epidemiological and pathological pattern of RHDV GI.1, which affects only rabbits older than 4 weeks of age (Liu et al., 1984), although there is isolated evidence of RHDV-RNA presence in hares (Lopes et al., 2014).

In areas where RHDV2 circulates, sympatric Iberian mesocarnivores come in contact with the virus, either by predation or necrophagy of infected wild rabbits or through contact with contaminated soil or vegetation (OIE, 2019). RHDV2-RNA was identified in both pine voles (*Microtus pinetorum*) and white-toothed shrews (*Crocidura russula*), two rodent species that are sympatric to the European wild rabbit (Calvete et al., 2019). The RHDV2 transmission to small mammals could happen due to their scavenging habits, or by ingestion of rabbit infected tissues or faeces (Calvete et al., 2019). Additionally, red foxes (*Vulpes vulpes*) (Chiari et al., 2016) and wolf (*Canis lupus*) (Di Profio et al., 2017) play a role as passive carriers, spreading European brown hare syndrome virus (EBHSV) by their faeces, after ingestion of infected hares.

Given this possibility, several sympatric species of wild animals such as birds, rodents, carnivores, including mustelids namely the Eurasian badger, have been investigated for RHDV2 at our laboratory over the last three years (*data not shown*). The Eurasian badger (*Meles meles*) is a gregarious, fossorial, and evasive species. Badgers are predominantly

nocturnal or crepuscular (Fedriani et al., 1999), mainly in the spring, when the wild rabbit activity peak coincides with the peak of RHD (Mutze et al., 2002). This trophic, opportunistic, generalist species preys on the European rabbit, particularly juvenile (Fedriani et al., 1999). In the summer and autumn/winter, lagomorphs represent about 60% and 22.7% of a badger's diet, respectively (Fedriani et al., 1999), whereas in the spring rabbit may account for up to 87.9% of the ingested biomass, according to a study carried out in Spain (Fedriani et al., 1999).

Another member of the *Lagovirus* genus, the rabbit calicivirus (RCV, GI.5) (Capucci et al., 1996) is an asymptomatic virus of the intestinal tract. In addition to these, the European RCV-E1 (GI.3) and Australian RCV-A1 (GI.4) (Strive et al., 2009; Le Gall-Reculé et al., 2011) are non-pathogenic rabbit viruses. The information on these viruses is scarce but can contribute as genetic donors resulting in recombinant pathogenic viruses (Silvério et al., 2018).

This study was part of a 3-years of monitoring haemorrhagic disease in the wild rabbits (Action Plan for the Control of Rabbit Haemorrhagic Disease Virus, Dispatch 4757/17 of 31st May), and sympatric species collected in mainland Portugal. Among several species investigated, some of the badgers tested RHDV2-positive by molecular methods. This finding prompted us to further investigate the presence of RHDV2 proteins, viral particles, and RHDV2 compatible lesions. To our knowledge, we are reporting for the first time the *Lagovirus europaeus* GI.4P-GI.2 crossing the barrier beyond the Lagomorpha order, namely to the Eurasian badger.

2. Material & Methods

2.1. Origin of the animals

A total of 10 European badgers were admitted for this study. All the information collected about these animals, namely sex, weight, date of collection, among others, is summarized in table S1 (Supplementary data).

One badger (B1) found dead on the road, and nine others (B2 to B10) found dead in agricultural areas, were collected during active prospection for wild rabbit carcasses and sympatric species, namely foxes, insects, birds and rodents, within the scope of an epidemiological evaluation of haemorrhagic disease in rabbit populations. All animals were found in the District of Santarém (Portugal NUT III, PT185 area).

The poor quality of the wildlife biological samples posed a major challenge to the laboratory diagnosis, which was overcome through the establishment of a comprehensive diagnosis strategy resourcing to several molecular, antigen detection methods, sequencing and transmission electron microscopy (TEM). Thus, the methodological strategy adopted was as follows; samples were tested by RT-qPCR (Duarte et al., 2015) and the negatives were excluded from further analyses. The RT-qPCR positive badgers showing milder autolysis were selected for RHDV2 sequencing analysis, immunohistochemistry (IHC) and TEM.

2.2. Necropsy sampling and histopathology

B1 was maintained at -20°C until a necropsy, while the remaining carcasses were kept at 4°C for a maximum period of 2 days. No badger was necropsied along with other species, namely rabbits, to avoid crossed contaminations. Necropsies were performed according to the routine implemented practices, as described in the necropsy manual (Peleteiro et al., 2016), and carried out at the Faculty of Veterinary Medicine, University of Lisbon (FMV-ULisboa, Lisbon, Portugal) or at the National Institute for Agricultural and Veterinary Research (INIAV I.P., Oeiras, Portugal).

Different samples were collected for molecular diagnosis, histopathology and bacteriology. To avoid faecal contamination, the sample collection was carried out in the following order: liver, spleen, kidney, lung, left ventricle, other organs, duodenum and finally faeces. Disposable material was used for each organ to avoid cross-contamination between matrices. Blood samples were not collected due to coagulation or autolysis.

For histopathology, liver, spleen, duodenum, stomach, kidney, lung, left ventricle, trachea, mesenteric lymph nodes were collected and fixated in 10% neutral buffered formalin,

routinely paraffin-embedded, sectioned at 3 μm, and stained with Hematoxylin and Eosin (H&E). Microphotographs were obtained with a DP23 Olympus digital camera.

Perls Prussian Blue was used to detect the presence of non-heme iron (ferritin and hemosiderin) in the tissues (Bancroft and Stevens, 1982).

2.3. Immunohistochemistry and dot blotting

Immunohistochemistry was performed as follows: (i) 4 μm sections of liver samples were mounted in appropriated glass slides (ii) deparaffinization and antigen retrieval was performed in a PT Link (Dako, Santa Clara, USA) at 96 °C for 20 min, with low pH EnVision FLEX target retrieval solution (code DM829; Dako, Santa Clara, USA); (iii) peroxidase block (with Peroxidase blocking solution, DAKO) was carried out for 20 min at room temperature; (iv) primary antibody (named pAb or Virlab derived from a hyperimmune serum collected from a rabbit infected in the facilities of the University of Oviedo (UniOvi, Oviedo, Spain) with strain RHDV-Ast89 (RHDV)), incubation diluted at the optimized concentration (1/1000) in Antibody Diluent (DAKO)) was incubated for 1 hour at room temperature; (v) incubation with the secondary antibody (at the concentration indicated by the manufacturer (Dako EnVision™+ Dual Link System-HRP, mouse anti-rabbit)) was carried out for 30 min at room temperature, (vi) staining was performed with DAB chromogen (DAKO) for 5 min, (vii) nuclei counterstain was carried out with Gills haematoxylin and finally (8) dehydration was done in an ethanol gradient before sections were mounted with a non-aqueous mounting medium. The necessary washes between incubations were performed with phosphate-buffered saline, pH 7.4 (PBS) twice for 5 min each with frequent manual agitation. The pAb was previously validated against RHDV and RHDV2 (González, 2019).

Dot blot was carried out using approximately 20% (w/v) homogenates prepared in PBS of liver and lung samples from badgers B5 and B6 after clarification at 6,000 g for 5 min. Liver homogenates from RHDV2-positive and RHDV2-negative rabbits were used as positive and negative controls, respectively. A grid was drawn on a piece of nitrocellulose membrane

(Thermo Fisher Scientific Inc., Waltham, USA) using a pencil. 1µl drops were deposited in the middle of the squares and the membrane was allowed to dry for 15 to 20 min at room temperature. The inhibition of nonspecific reactions was performed by shaking incubation with 5% milk powder in PBS (w/v) for 45 min at room temperature. Two 5-minute washes with shaking were performed with 0.05% Tween 20 (v/v) in PBS. Then, the membranes were incubated for 1h at room temperature with agitation with primary antibodies diluted at the optimized concentrations in 0.05% Tween 20 in PBS. Two monoclonal antibodies (mAb) were used, namely 1A2 (anti-VP60, Ingenasa, Madrid, Spain) and 3A10 (anti-VP60 of RHDV and RHDV2, S domain, produced in the Department of Biochemistry and Molecular Biology (UniOvi)). The polyclonal antibody (pAb) was also used. After incubation, two additional washes were performed as described above. The membranes were then incubated in the dark under shaking conditions with the secondary antibody, goat anti-rabbit IgG, conjugated with fluorescein isothiocyanate (FITC) (Merck Life Science S.L.U. suc, Lisbon, Portugal) for the polyclonal serum or anti-Mouse IgG (whole molecule)–FITC antibody produced in goat (Sigma-Aldrich, United States of America) for the monoclonal antibodies, both diluted at 1:200 in Tween 0.05% in PBS for 1 hour, at room temperature. Finally, after two wash steps of 5 min each, visualization of membranes was carried out using Odyssey Infrared Imaging System (LI-COR Biosciences, Nebraska, USA) and the software Image Studio (LI-COR Inc., Nebraska, USA).

2.4. Immunofluorescence

Tissue samples from B5 and B6 were embedded in optimal cutting temperature (OCT) compound and sections were cut onto slides using a cryostat at -20°C. The cryostat sections were permeabilized using 0.2% saponin in PBS (w/v) for 20 min before emerged in blocking solution (0.02% saponin, 1% BSA in PBS) for 30 min at room temperature. Antibody labeling was performed by incubating sections with pAb (polyclonal antibodies) and the mouse monoclonal anti-LAMP1 antibody (ab25630, Abcam, Cambridge, UK) in blocking solution for 2 hours at room temperature. Secondary antibodies used at 1:500 (Goat anti-Rabbit IgG (H+L) Cross-Adsorbed Secondary Antibody, Alexa Fluor 488 (ThermoFisher A-11008) and Goat anti-Mouse IgG (H+L) Cross-Adsorbed Secondary Antibody, Alexa Fluor 555

(ThermoFisher A-21422)) and in some cases, fluorescent phalloidin (ab176759, Abcam) were added to the sections and incubated for 1 hour at room temperature. Finally, coverslips were added to the slides using mounting media containing DAPI (ab228549, Thermo Fisher Scientific Inc., Waltham, USA). Images were acquired in a Leica SP8 confocal microscope and grey-scale inverted images were produced using ImageJ (NIH, Bethesda, USA). Negative controls were either uninfected or infected samples where the polyclonal antibody was omitted.

2.5. Molecular diagnosis of RHD, sequencing and phylogenetic analysis

The tissue and faeces samples were homogenized at 20% in sterile PBS (w/v)), using mechanical homogenization with 0.5 mm zirconium beads (Sigma-Aldrich, United States of America) and the FastPrep FP120 Bio101 Homogenizer (Level 5 velocity, 45s, Savant Instruments, India) and total nucleic acids extracted from 200 μL supernatant after a 5 min 6,000g centrifugation. The automatic extraction was performed with the MagAttract 96 cador Pathogen kit (Qiagen, Germany) on the BioSprint 96 automatic extractor (Qiagen, Germany), following the protocol supplied with the kit.

Each tissue and faecal sample was tested for RHDV2-RNA (GI.2) by a specific RT-qPCR developed by Duarte et al. (2015) that targets a 125 nt region of the VP60 gene, using the OneStep RT-PCR Kit (Qiagen, Germany).

cDNA was synthesised with the SuperScript™ IV First-Strand Synthesis System (InVitrogen) according to the manufacturer's recommendations, using either oligo(dT)$_{12-18}$ and random hexamers.

The conventional RT-PCR (Dalton et al., 2018) for differentiation of RHDV2 strains from RHDV2 recombinants was carried out using the Phusion Flash High-Fidelity PCR Master Mix (Thermo Fisher Scientific Inc., Waltham, USA) according to the manufacturer's recommendations.

For two positive liver samples (B5 and B6), amplification of the partial RdRp gene and full VP1 (VP60) gene sequence was accomplished using the primers described in Table S2 of

supplementary data, where all the primers used in this investigation are shown. Regarding the other samples, partial sequencing (table S1) was performed to confirm the presence of RHDV2.

The amplicons were purified using the NZY GelPure kit (NZYTech, Lisbon, Portugal), following the manufacturer's instructions, and directly sequenced with a 3130 Genetic Analyser (Applied Biosystems, California, USA). The resulting sequences were analysed using Seqscape software v2.7 (Applied Biosystems, California, USA). Merged and assembled consensus sequences were submitted to GenBank.

The partial sequence of RNA polymerase (RdRp) gene and the complete vp60 gene sequence from badger B6 were compared with reference strains for all known RHDV and RHDV2 genotypes and variants that infect the European rabbit for which this genomic region is available in the database. The accession numbers are shown in the phylogenetic tree (Figure 16). The alignment was achieved using the Mega X, for a total of 2191 positions (partial RdRp gene and complete VP60 gene) and the evolutionary history inferred using the Maximum Likelihood method and General Time Reversible model (Nei and Kumar, 2000). The model was selected using the Mega Function having selected the model GTR+G+I (BIC 37184.06 and AIC 36028.07).

The known principal genotypes and variants of *Lagovirus* that can infect the *Oryctolagus cuniculus* are shown in the figure, as reference. The tree with the highest log likelihood (-17929.21) is shown.

2.6. Transmission electron microscopy

Transmission electron microscopy (TEM) was performed in liver samples from three badgers (B1, B5 and B6). Briefly, samples were fixed for 72h with a solution 0.1M sodium cacodylate (Sigma-Aldrich, USA) containing 2.5% glutaraldehyde (Sigma-Aldrich, USA). The regions of interest were sliced in small ~1mm3 and washed 5 times in 0.1M sodium cacodylate buffer, samples were then post-fixed with 1% osmium tetroxide (EMS, Hatfield, UK) for 1 hour, and en bloc stained with 1% Millipore-filtered uranyl acetate (Agar scientifics, Stansted, UK). Samples were dehydrated in increasing concentrations of ethanol, infiltrated and embedded

in EPON 812 (EMS, Hatfield, UK). Polymerization was performed at 60°C for 24 hours, and ultrathin sections were obtained in a Reichert ultracut E ultramicrotome (Leica, Wetzlar, Germany), collected to 1% formvar coated copper slot grids (Agar scientifics, Stansted, UK), stained with 2% aqueous uranyl acetate and lead citrate and examined in a Jeol 1400plus transmission electron microscope at an accelerating voltage of 120 kV. Digital images were obtained using an AMT XR16 bottom mid mount digital camera (AMT, Woburn, USA). The sections were systematically analysed using AMT© software and several high and low magnifications were acquired

2.7. Other virological analyses

Tissue and faeces samples were homogenized and total nucleic acids extracted as described above. Feline and canine Parvoviruses, canine distemper virus (morbillivirus), mammal (canine, feline and porcine) coronaviruses, type A rotavirus, Ausjesky Disease Virus and other herpesviruses were investigated using the methods and matrixes described in table S3.

2.8 Bacteriological analysis

Liver, spleen, kidney and lung from B5, B6, B7 and B8 badgers were collected at necropsy for bacteriology using conventional techniques. In the case of B5 and B6, all samples were processed separately. A pool of organs from the animal was prepared for B7 and B8. The remaining badgers were not sampled for bacteriology due to extensive autolysis or faecal contamination.

Briefly, aerobic bacteria isolation was performed on Columbia agar supplemented with 5% sheep blood (BioMérieux, Lisbon, Portugal) and MacConkey agar (Thermo Fisher Scientific Inc., Waltham, USA), incubated at 37°C for 24 to 48 h. Strict anaerobic bacteria isolation was performed on Schaedler agar supplemented with 5% sheep blood (BioMérieux) and incubated for 48 h at 37°C in the absence of oxygen. Afterward, isolates were identified through their macro- and microscopic morphology, staining characteristics and biochemical profiling using API (BioMérieux) galleries, according to the manufacturer's instructions.

2.9. Parasitological analysis

Faeces were collected for the flotation method to detect helminth eggs or protozoan oocysts. Faeces were mixed with saturated sugar solution (1:4) and, after pouring the solution into tubes, lamellae were placed on their top to allow adhesion to the glass and allowed to stand for 15 minutes. Lamellae were then transferred to slides and preparations were observed with a compound microscope.

Gastrointestinal content was also collected and placed on a tray with a black background, filled with warm water and, after standing for a few minutes, supernatant was removed by decantation. This procedure was repeated three times until the liquid became clear enough to visualize the presence of helminths by contrast. Furthermore, flotation method for egg and oocysts detection was also performed as described above.

3. Results

3.1 Necropsy data

Necropsy of badger B1 revealed a good overall body condition, multiple fractures of the skull and lacerations in the liver and spleen, interpreted as resulting from a traffic accident. The autolysis limited the interest in the identification of the lesion, both grossly and microscopically. B2, B3, B4, B9 and B10 presented severe autolysis, good body condition, and no visible lesions. Badgers B5 and B6 were emaciated, severely dehydrated, with uncoagulated blood, congestive foci in the lungs and with the liver slightly discolorated. B7 and B8 presented similar lesions, however with coagulated blood. Other data from the necropsies are shown in Supplementary Table S1 available as supplementary data.

3.2. Histopathological findings

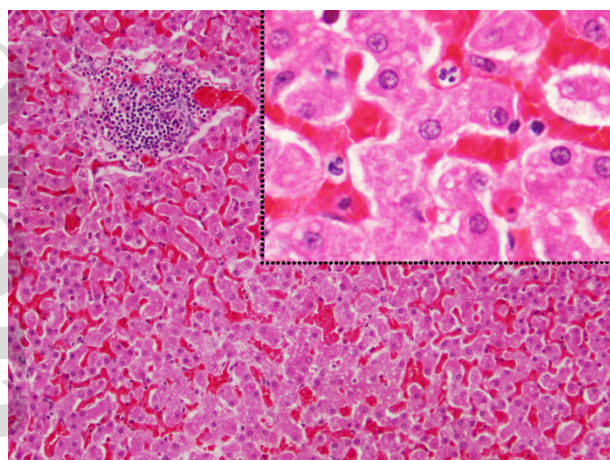Histopathology data for badgers B5 to B8 is summarized in Table 1, and the main findings shown in figures 1 to 10.

Figure 1. Liver (B6). Mild hydropic degeneration of the hepatocytes in the lower centre. Focal infiltration of mononuclear cells in the upper left. The hydropic degeneration can be seen at higher magnification in the inset. H&E, x 100, inset, x 400.
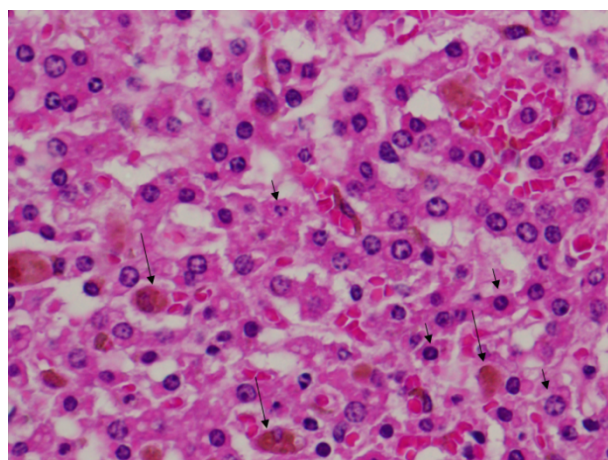

Figure 2. Liver (B8). Hydropic degeneration of the hepatocytes. Some cells show pyknosis and karyorrhexis (short arrows), as well as hyperchromatosis of the nuclear membrane; oedema of the perisinusoidal space and Kupffer cells containing hemosiderin (long arrows). H&E, x 400.
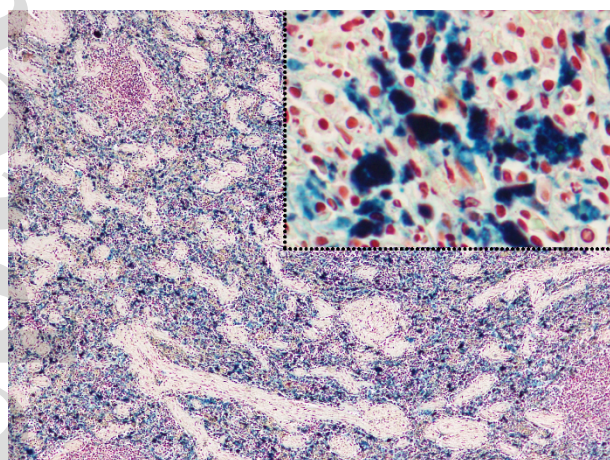
Figure 3. Spleen (B8). Marked presence in the red pulp of hemosiderin containing macrophages. Perls Blue, x 40, inset x 100.
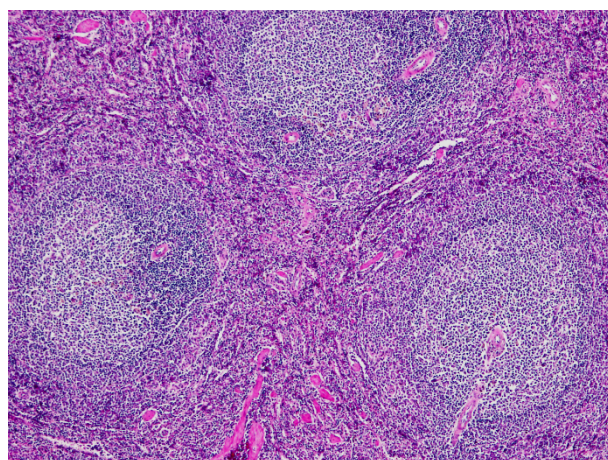

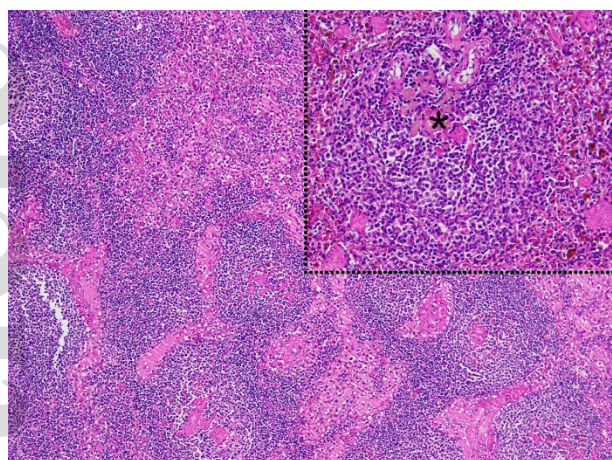**Figure 4.** Spleen (B6). Hyperplasia of the lymphoid follicles. H&E, x 100.

Figure 5. Spleen (B8). The center of some lymphoid follicles shows focal deposits of acidophilic material (*). H&E, x 40, inset x 100.
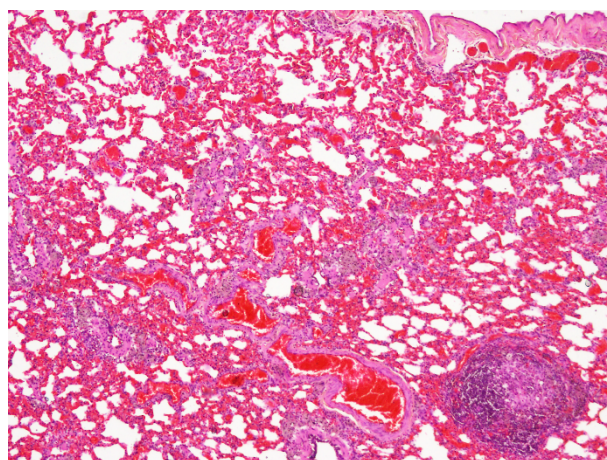

Figure 6. Lung (B6). Severe diffuse congestion of the alveolar septa some of which are thickned due to inflammatory cell infiltration. Granuloma in the lower right. H&E, x 40.
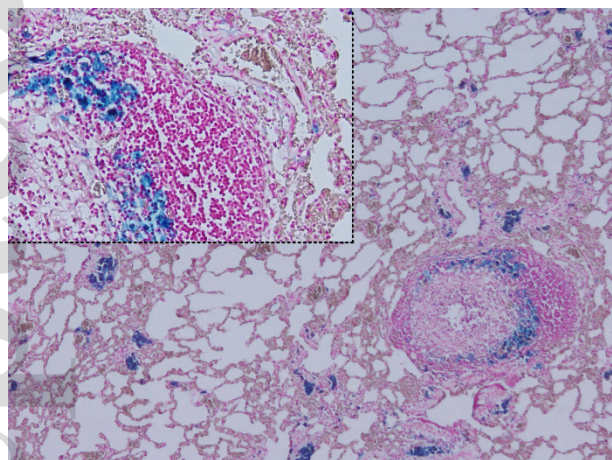

Figure 7. Lung (B6). Iron deposits in the alveolar septa and in macrophages in the periphery of a granuloma. Perls Blue, x40, inset x100.
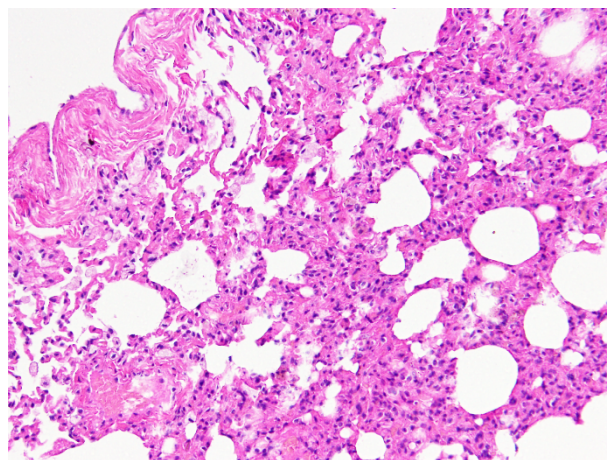

Figure 8. Lung (B8). Diffuse interstitial pneumonia. The pleura is corrugated. H&E, x 100.
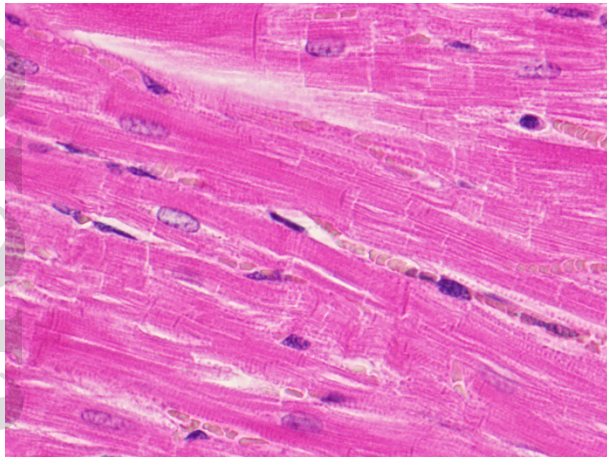
Figure 9. Myocardium (B5). Striation loss and granular appearance of the cardiomyocites. H&E, x 400.
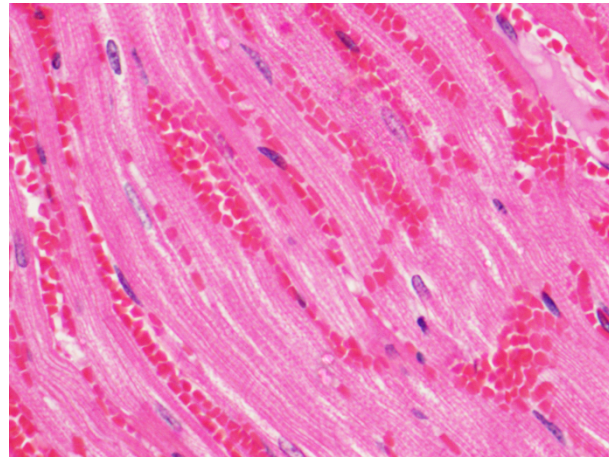

Figure 10. Myocardium (B6). Focal intercellular hemorrhage. Striation loss and granular appearance of the cardiomyocites. H&E, x 400.

Liver (3 out of 4) showed areas of hepatocellular hydropic degeneration, and individual cell necrosis (Figures 1 and 2). In two cases, generalized moderate oedema do the perisinusoidal space (space of Disse) was evident. Kupffer cells containing hemosiderin were identified in two cases.

Spleen showed hemosiderin-laden macrophages in the red pulp in most cases. This was marked in two cases, posteriorly demonstrated with Perls Blue stain for iron (Figure 3) and mild to moderate in all others. In two badgers, white pulp hyperplasia was also seen (Figure 4). In one case, not coincident with the lymphoid hyperplasia, focal deposits of acidophilic material (fibrin -like) were present in germinal centres (Figure 5).

In the lungs, severe congestion of interalveolar septa was present in two cases (Figure 6). Small aggregates of hemosiderin-containing macrophages were detected in the interalveolar septa in one case (Figure 7). In two badgers, interalveolar septa were thickened due to marked to moderate infiltration of mononuclear inflammatory cells (diffuse interstitial pneumonia) (Figure 8).

In the kidneys, vacuolar and granular degeneration of tubular cells in the proximal and distal tubules were present in all cases. In some of these tubules, necrosis of tubular cells was evident. In the heart, cardiomyocyte degeneration consisting of loss of striation and granular appearance of the cytoplasm was evident (Figure 9). In one case this was accompanied by focal haemorrhage (Figure 10).

Table 1- Histopathological findings in badgers B5, B6, B7 and B8

ID	Liver	Spleen	Lung	Kidney	Others
B5	Hepatocytes with minimal changes. In some areas, they show mild hydropic degeneration.	Accumulation of hemosiderin-laden macrophages in the red pulp. Mild hyperplasia of lymphoid follicles, which show foci of acidophilic material compatible with fibrin in the germinal centers.	Thickening of interalveolar septa with infiltration by mononuclear inflammatory cells (diffuse interstitial pneumonia). Frequent aggregates of hemosiderin-laden macrophages. Vicarious alveolar emphysema. Shrinked pleura.	Vacuolar and granular degeneration of epithelial cells in the proximal and distal tubules.	Cardiomyocytes granular degeneration and loss of striation. Thymus: necrosis of 10-15% of lymphocytes, which show karyolysis and kariorrexis.
B6	Severe congestion. Hepatocytes with generalized and severe hydropic degeneration. About 50% of the hepatocytes show no nucleus (kariolysis).	Hyperplasia of lymphoid follicles. Diffuse infiltration of red pulp by mononuclear cells (chronic splenitis).	Severe congestion and moderate thickening of alveolar septa by mononuclear inflammatory cells (interstitial pneumonia). Frequent aggregates of hemosiderin-laden macrophages. Vicarious alveolar emphysema.	Congestion of the cortex. Necrosis of tubular epithelium of proximal and distal tubules.	Cardiomyocytes granular degeneration and loss of striation. Haemorrhagic foci.
B7	Occasional hyperchromatosis of the nuclear membrane, karyorrhexis and picnotic nuclei. Space of Disse oedema with mild atrophy of hepatocytes.	Lymphoid follicles hypoplasia and fibrotic changes of the red pulp (chronic splenitis).	Severe congestion and moderate thickening of alveolar septa by mononuclear inflammatory cells (interstitial pneumonia). Vicarious alveolar emphysema.	Vacuolar and granular degeneration of epithelial cells in the proximal and distal tubules.	Cardiomyocytes granular degeneration and loss of striation.
B8	Generalized hepatocyte hydropic degeneration. Occasional hyperchromatosis of the nuclear membrane, karyorrhexis and picnotic nuclei. Intralobular Kupffer cells containing hemosiderin. Space of Disse oedema.	Accumulation of hemosiderin laden macrophages in the red pulp. Lymphoid follicles show small deposits of acidophilic material compatible with fibrin in the germinal centers together with hemosiderin laden macrophages.	Thickening of interalveolar septa with infiltration by mononuclear inflammatory cells (diffuse interstitial pneumonia).	Vacuolar and granular degeneration of epithelial cells in the proximal and distal tubules.	Cardiomyocytes granular degeneration and loss of striation.

3.3. Immunohistochemistry and Dot blot

To investigate the presence of the virus in the tissues, detection of the viral capsid protein (mainly composed by VP60) was attempted in the badger and rabbit tissues by immunolabelling techniques using polyclonal (pAb) and monoclonal antibodies (1A2 and 3A10).
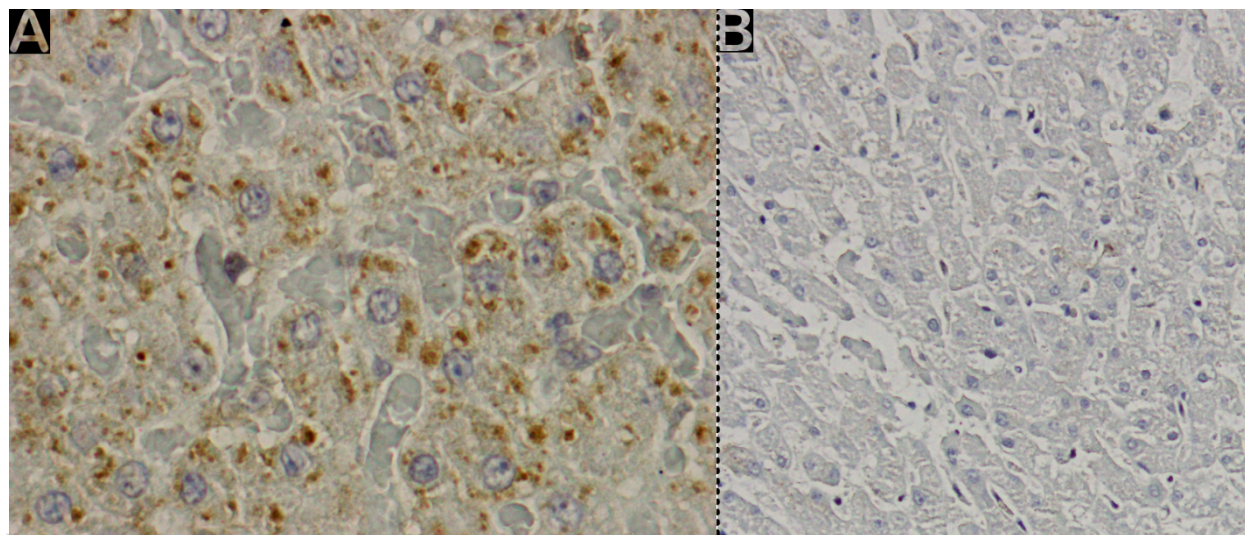

Figure 11. Immunostaining for RHDV2 in the liver of badger B5 (left). Hepatocytes show cytoplasmic granular brown staining. At right, negative control of a non-infected badger liver. DAB counterstained with Gills hematoxylin, x400.
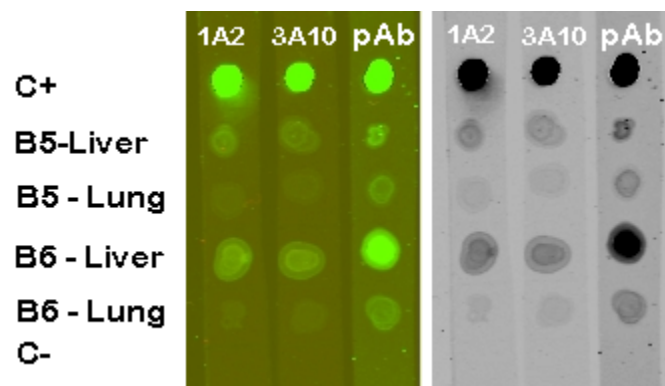
Figure 12. Dot blots from B5 and B6 badgers.C+ homogenate from a RHDV2 positive rabbit. C - Bovine serum albumin.

Immunohistochemistry of badgers' livers carried out with the pAb against RHDV, allowed the observation of generalized cytoplasmic staining of the hepatocytes of badgers B5 (Figure 11) and B6 (showing similar staining, result not shown), contrarily to the absence of staining in liver samples from a qPCR- negative badger and a qPCR-negative rabbit,

(*results not shown*). In addition to cytoplasmic staining in badgers B5 and B6, some hepatocytes also showed nuclear staining.

The same positive reaction for badgers B5 (weaker) and B6 (stronger) was observed in the dot blot analysis (Figure 12). Like in immunohistochemistry, in the dot blot, the pAb generated stronger reactions.

3.4. Immunofluorescence

To further demonstrate replication of RHDV2, indirect immunofluorescence was performed in the liver of badgers B5 (named #1) and B6 (named #2). We observed encapsulated virions, recognizable by the FITC-antibody directed to VP60, whose density is compatible with active replication of RHDV2 in the tissues (Figure 13). DAPI staining was used for labeling DNA in fluorescence microscopy and phalloidin to stain the actin filaments. Livers from an RHDV2 infected rabbit and the RHDV2 non-infected badger were used as a positive and negative control, respectively.
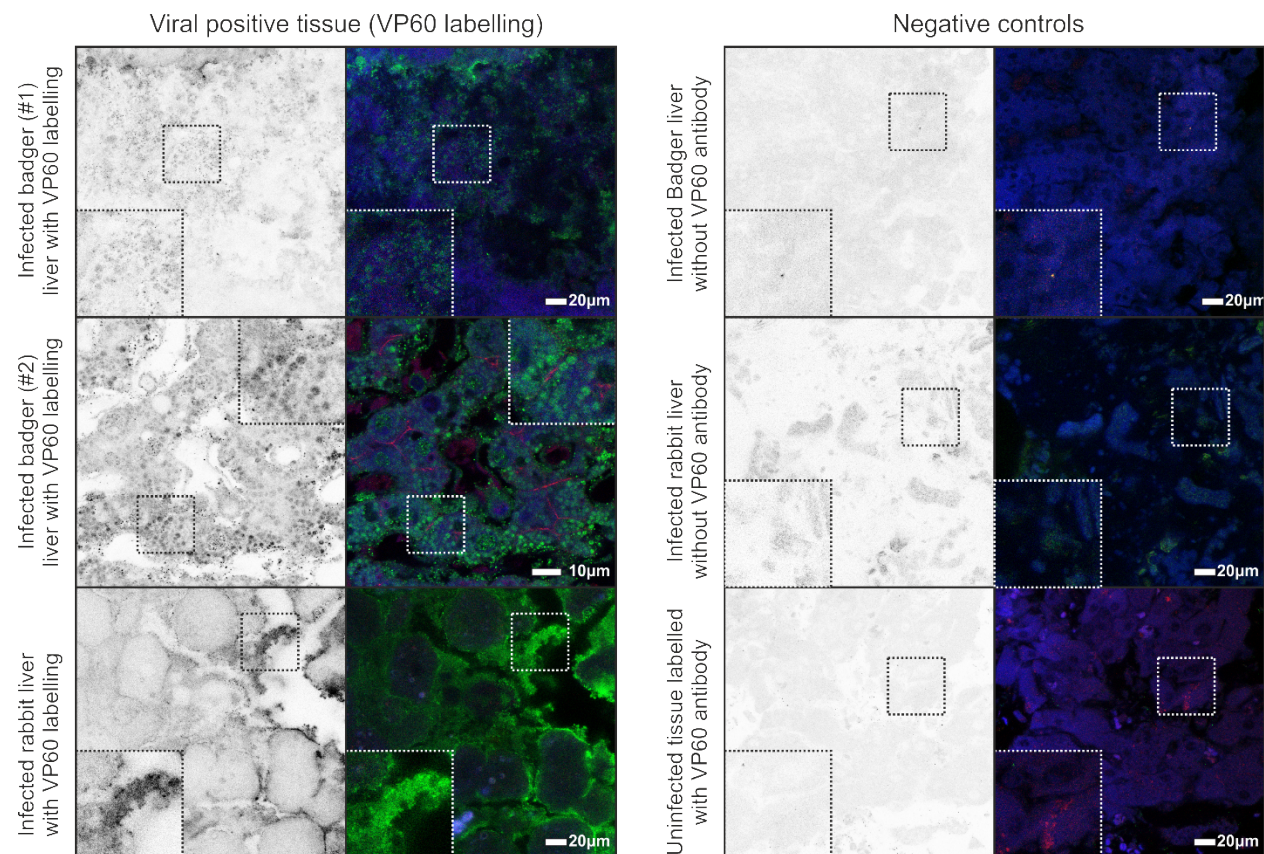
Figure 13. Immunoflorescence using Virlab polyclonal antibody to detect viral protein (green), DAPI staining was used to detect DNA (blue) and phalloidin staining to detect actin filaments (red). All the figures present the gray-scale/inverted contrast at the left and the original view at the right.

A clear green labbelling is observed in both badgers' livers, and the positive rabbit sample. The badgers' samples showed distinct punctate staining (more evident in the B6), ascribing virus localisation to subcellular compartments. Due to the tissue

preservation conditions, DAPI is dispersed by the cytoplasm of cells. For the same reason, phalloidin is sometimes also difficult to observe.
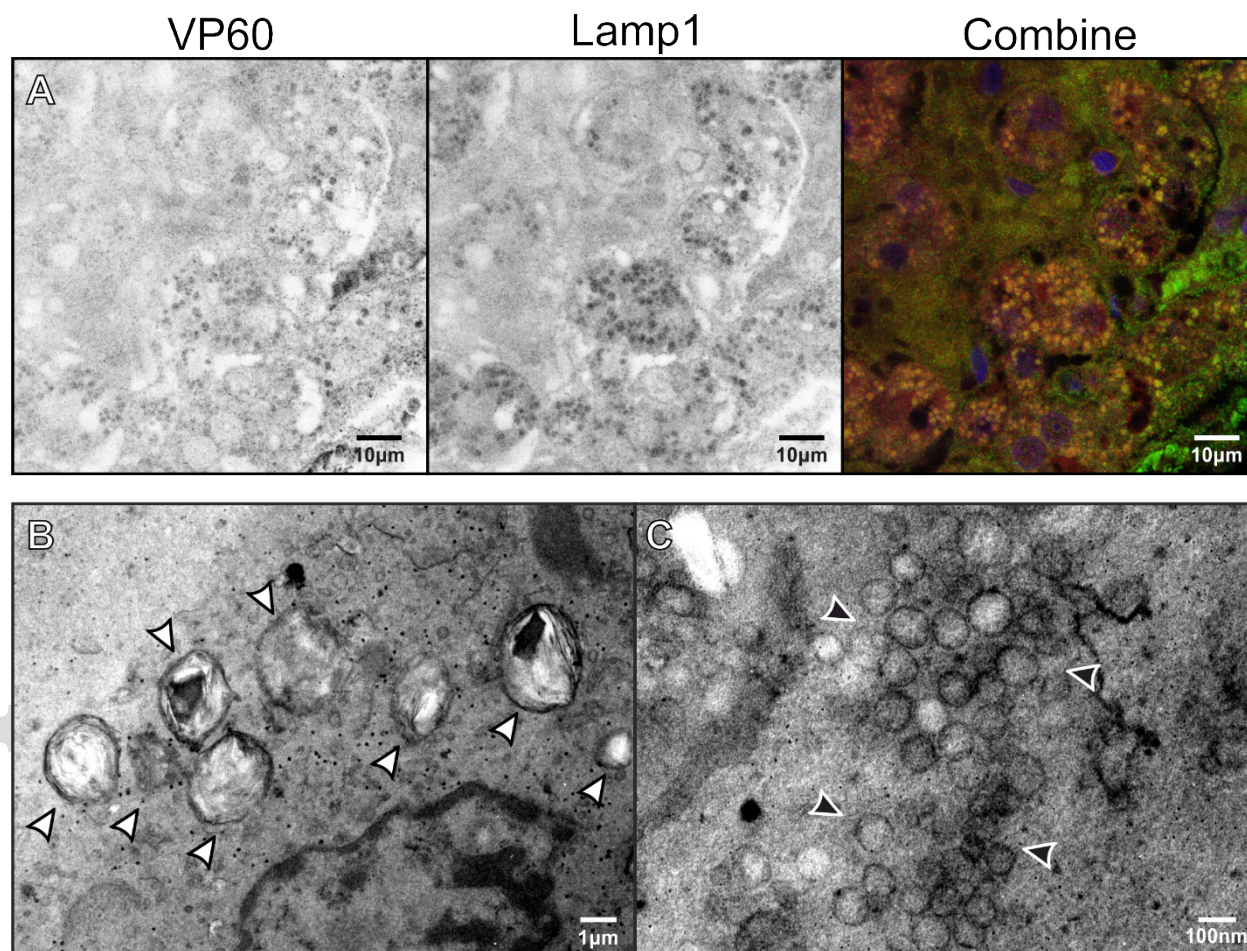
VP60   Lamp1   Combine

Figure 14. Immunolabelling of viral protein VP60 (A-left, grayscale), LAMP 1 (A-middle, grayscale), and combined (A-right). (B) Transmission electron microscopy showing clusters of lysosomal like structures (white arrowheads) within hepatocytes of badger (B5). (C) vesicles (black arrowheads) were also observed in the hepatocytes of badger B5.

To evaluate the presence and increment of lysosomal or autophagosome-like structures that are usually associated with viral factories, LAMP 1 fluorescence staining was performed. The membrane glycoprotein 1 was detected by direct immunofluorescence (Figure 14 A) in the cytoplasm of infected hepatocytes. The presence of a large number of lysosomes was also confirmed in hepatocytes of RHDV2 infected badgers (B1, B5 and B6) by TEM showing that viral particles colocalize with lysosomal structures, indicating that the virus is within lysosomes (Figure 14 B and C).

3.5. Molecular diagnosis and sequencing analysis

RHDV2-RNA was detected by RT-qPCR in most of the organs from badgers B1, B5–B10 (Table 2), suggesting that the virus was disseminated systemically. In general, the higher viral loads were observed in the liver and spleen (Table 2). None of the badgers tested positive for RHDV GI.1-RNA.

Table 2 – RT-qPCR amplification results and respective estimated viral loads per mg of tissue.

* according to the quantitative method described by Duarte et al., 2015. NT-not tested, ND-not detected;

Darker cells correspond to higher viral loads

Full RHDV2 vp60 sequences were obtained for badgers B5 and B6 showing these to be RHDV2 strains (GI.2). Despite for badgers B1, B7 to B10 the vp60 gene was not sequenced, the specificity of the RT-qPCR method used (Duarte el al. 2015) allowed to the conclusion that all strains were also GI.2.

To further investigate the genomic composition of the RHDV2 badgers' strains, an upstream genomic region comprising the 3' end of the RdRp gene was amplified by a conventional RT-PCR (Dalton et al., 2018) and sequenced.

These partial RdRp nucleotide sequences from badgers B1(MW446907), B5(MT610362), B6(MT610363), B7(MW446908), B8(MW446909), and B9(MW446910) showed them to be all GI.4 strains regarding the non-structural genes.

*Viral copies/mg tissue *

Organs	B1	B2	B3	B4	B5	B6	B7	B8	B9	B10
Liver	1.65×10^4	ND	ND	ND	2.99×10^6	1.14×10^4	1.69×105	2.84×10^4	2.09×10^5	6.02×10^5
Spleen	3.68×10^3	ND	ND	ND	4.25×10^5	1.66×10^6	5.53×10^5	3.34×10^4	5.01×10^5	1.92×10^5
Heart	7.13×10^4	ND	ND	ND	1.56×10^3	1.18×10^5	3.16×10^3	ND	8.14×10^2	4.57×10^3
Lungs	1.57×10^6	ND	ND	ND	1.21×10^6	5.15×10^3	5.78×10^2	1.19×10^3	1.67×10^3	ND
Duodenum	9.78×10^4	ND	ND	ND	3.31×10^3	4.75×10^5	7.47×10^4	5.50×10^3	8.67×10^3	1.75×10^4
Kidney	ND	ND	ND	ND	3.07×10^4	5.15×10^3	7.57×10^4	ND	5.63×10^2	8.90×10^3
Faeces	ND	ND	ND	ND	1.10×10^3	1.57×10^5	ND	ND	3.66×10^3	1.74×10^4
Mesenteric lymph node	NT	NT	NT	N	NT	NT	3.44×10^4	3.34×10^4	NT	NT

The final 2,188 nucleotide sequences obtained from badger B5 (MT610362) and badger B6 (MT610363) were aligned and compared, showing 100% identity with each other. BLAST search (performed on 05th January 2021) using the VP60 sequence showed higher similarities, namely 99.37% and 98.10% with MG763954 (a recombinant strain reported in 2018 from a wild-rabbit collected in Estremoz, south Portugal), and KF442963 (also a recombinant strain obtained in 2013 from a wild rabbit from in Barrancos, south Portugal), respectively. The BLAST analysis of the RdRp partial sequences of B5 and B6 showed higher identity with the same sequences, namely 97.54% with sequence MG763954.

The partial RdRp nucleotide sequences (409nt long) from badgers B5 and B6 shared 95% of identity with B1, 83% with B7 and B8, and 82% of identity with B9.

The amino acid sequence of the partial RdRp (149 residues long) deduced from sequence MT610363 (B5) showed 98.66% identity with the homologous region from sequence AIT40572.2 (RHDV2 collected from a wild rabbit from Estoi, Faro, south of Portugal in 2013). Also, the complete amino acid sequence of VP60 gene (579 residues long) deduced from sequence MT610363, showed 99.83% identity with the VP60 sequence from a strain collected from Valpaços, Vila Real Portugal in 2012 (AJE29738).

When the deduced amino acid sequences comprising the contiguous partial RNA-dependent RNA polymerase gene and complete VP60 gene were compared with the GenBank database, the greatest identity (99.59%) was found with sequence AIT40572.2. With regards to this sequence, three amino acid substitutions were observed in the RHDV2 badger sequence MT610363, namely an Ala^{1648} to Thr^{1648} (a radical amino acid residue change) and a Tyr^{1737} to His^{1737} (conservative replacement) in the RdRp protein, and one substitution in the VP60 protein, namely a Thr^{2109} to Ser^{2109} (conservative

replacement), located in loop L2 of P2 sub-domain (positions indicated refer to the polyprotein). These three aa residues found in the badger polyprotein are not unique in badgers' strains, being also found in rabbits' strains.

3.6 Phylogeny of the badgers' RHDV2 strains

The 2,191-nt long region containing the partial RdRp gene and full VP1 (VP60) gene sequences from badger B5 (MT610362) and B6 (MT610363) were used to assess the phylogenetic relationships between these strains and the RHDV and RHDV2 strains from wild rabbits by Maximum Likelihood (ML) (Figure 15).

As expected, the badger strain was grouped with Portuguese recombinant strains, close to the reference strain RCV-A1-like/RHDV2, with GI.2 VP60 genotype and variant of GI.4 of polymerase gene. The access numbers of the sequences included in the tree are shown in the phylogenetic tree (Figure 15).
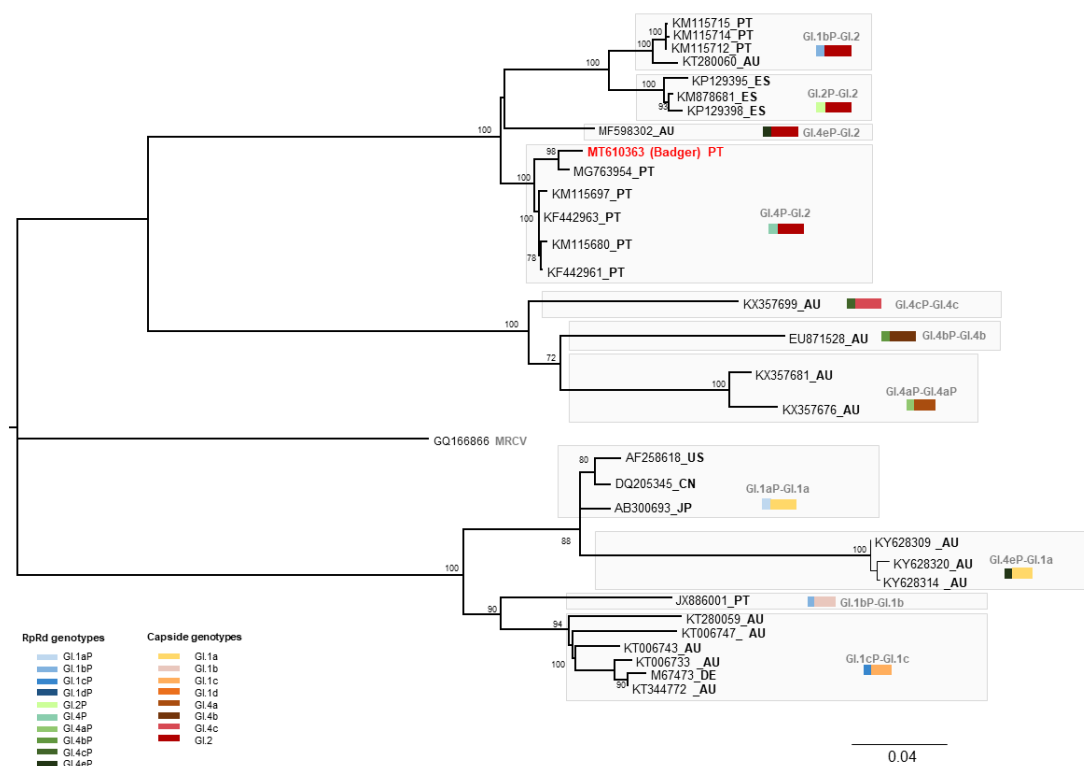
Figure 15. Unrooted phylogenetic tree inferred by using the Maximum Likelihood method and General Time Reversible model (Nei and Kumar, 2000). The tree with the highest log likelihood (-13922.65) is shown. A discrete Gamma distribution was used to model evolutionary rate differences among sites (5 categories (+G, parameter = 1.4546)). The rate variation model allowed for some sites to be evolutionarily invariable ([+I], 50.56% sites). The tree is drawn to scale, with branch lengths measured in the number of substitutions per site. This analysis involved 32 nucleotide sequences. Codon

positions included were 1st+2nd+3rd+Noncoding. There were a total of 2191 positions in the final dataset. The analyses were conducted in MEGA X (Kumar et al., 2018), and the tree was edited with FigTree software V1.4.4

3.7. Transmission Electron Microscopy

Viral particles were identified by transmission electron microscopy (TEM) in liver of badgers B1, B5, and B6. Virions showed the typical icosahedral morphology and size was of 33.4nm±4.1nm (mean±SE, 30 measures, Figure 16) compatible with RHDV particles whose diameter is reported to be from 27 to 40 nm (Ohlinger et al., 1990; Capucci et al., 1991).

The virions were detected in the nucleus and cytoplasm of hepatocytes, in the interstitium of liver, lung, and heart, and in the cytoplasm of liver Kupfer cells. A badger (unnumbered), negative for RHDV2 on qPCR was used as negative control; no virion-like structures were observed.
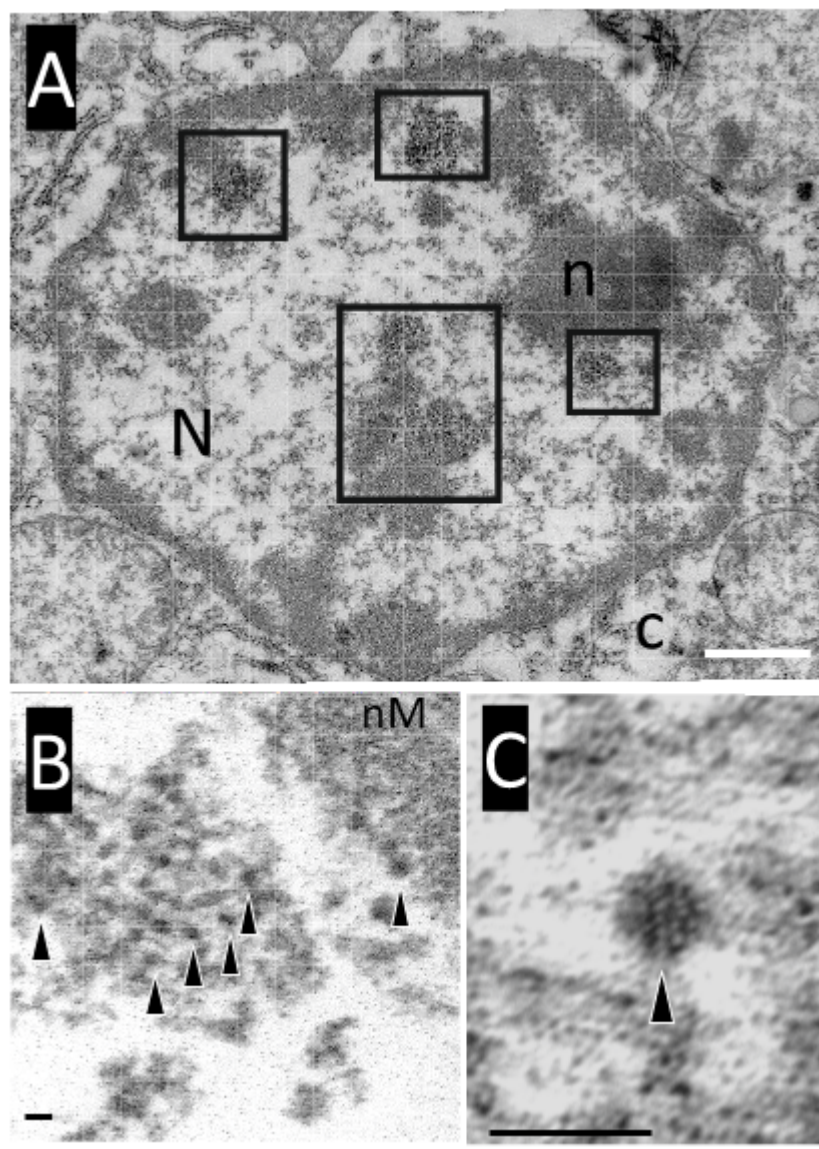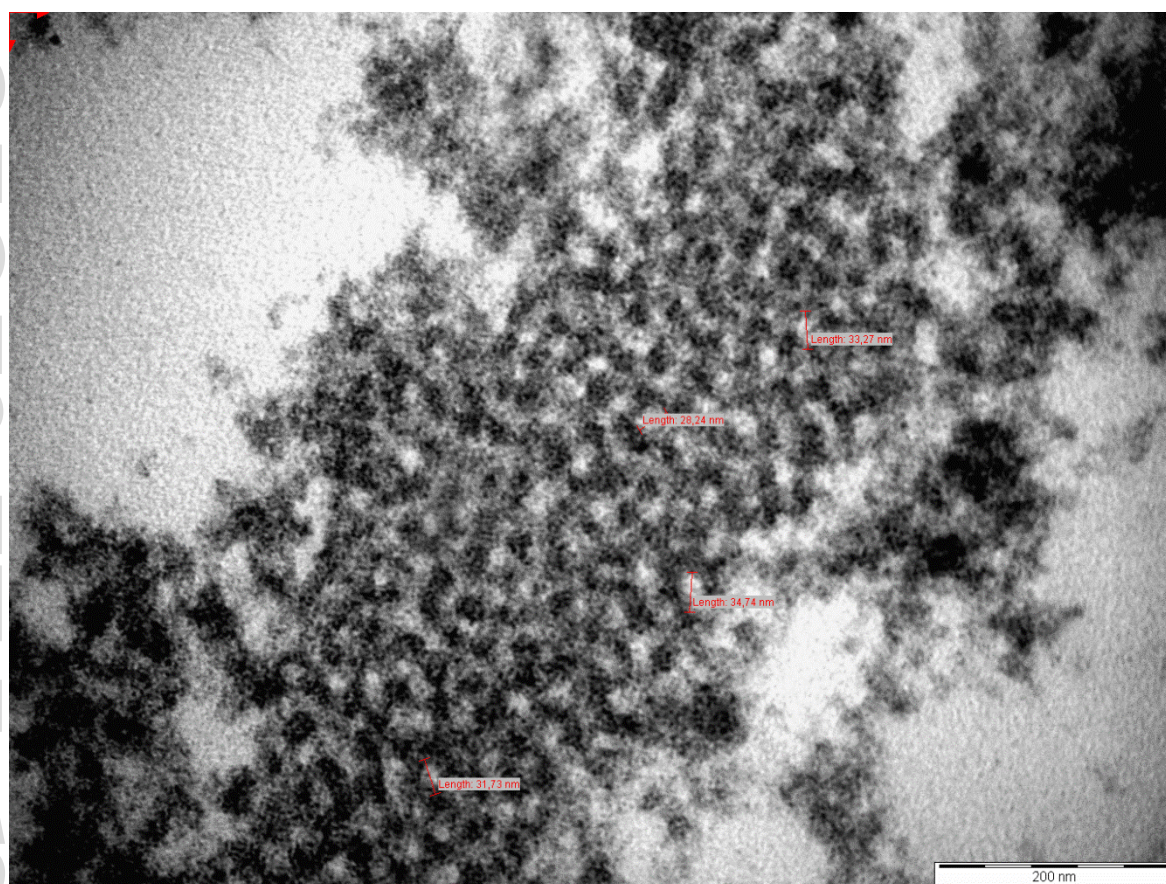
Figure 16. Transmission electron micrographs of badger B5 liver. A. Low magnification showing the nucleus (N) of an hepatocyte, with an eccentric nucleolus (n), showing several clusters of viral particles (insets). B. High magnification of the nucleus showing clusters of particles (arrow heads), which differ from neighboring cromatin (c) adjacent to nuclear membrane (nM). C. Detail of a viral particle (arrowhead) suggesting an octagonal shape. Bars: 1µm (white bar), 50nm (black bar). D. High magnification of a apparent intranuclear viral factory, with viral particles measuring from 26 to 38 nm compatible with caliciviruses. Bar: 200 nm.

3.8 Virological analyses besides RHDV2

None of the badgers tested (B1, B5 to B10) was positive for all the other viruses tested.

3.9. Bacteriological analysis

Low numbers of *Micrococcus* sp. and *Staphylococcus sciuri* were isolated from the liver and lung of badger B5. The remaining organs showed no aerobic or anaerobic bacterial growth. Regarding badger B6, *Escherichia coli* was isolated from the liver and spleen, and low numbers of *Clostridium* sp. from the liver, spleen and kidney.

In the samples collected from badgers B7 and B8 low quantities of *Klebsiella oxytoca* and *Klebsiella pneumonia* ssp*. pneumoniae* were isolated, respectively*.* No *Mycobacterium* spp. was detected in the badgers.

3.10. Parasitological anaylsis

No ecto or endoparasites were found in badgers B1, B7 and B8. In Badger B6, fleas were identified as *Pulex irritans*. For badgers B5 and B6, hookworm eggs were found through the flotation method. In the later adult forms of hookworms (Family Ancylostomatidae) were also detected during the analysis of the gastrointestinal content. *Isospora* spp., *Uncinaria criniformis* and nematodes from Capillariidae family were identified in badger B6, and *Capillaria* sp. in badger B10.

4. Discussion

Our work was conducted in the scope of a national surveilance program for RHDV2 in wild rabbits and sympatric species (Dispatch 4575/17, 30 may MAFDR). As sympatric species, European badgers were also included in the monitoring program, which is why those found dead were sampled for investigation. However, the poor quality of these opportunistic biological samples poses major challenges to the laboratory diagnosis, overcome through the establishment of a comprehensive diagnosis strategy combining several molecular and antigen detection methods, sequencing analysis and electron microscopy observation. The serological investigation was not possible due to the lack of fresh blood samples.

The methodological strategy adopted for this study was as follows: tissue samples were firstly tested by RT-qPCR (Duarte et al., 2015) allowing the selection of the positive badgers for further analyses. Of these, only the badgers showing milder autolysis were elected for RHDV2 sequencing analysis, IHC and TEM. The exception was made for badger B1, the

only material available for the first two years of this investigation, and for which, tissues were used for testing, despite severe autolysis.

To exclude the possibility of the microscopic lesions being a consequence of other infectious agents rather than RHDV2, samples were tested for additional pathogens. Several potential Eurasian badger viruses (canine distemper virus, canine and feline parvovirus, canine, feline and porcine coronaviruses, type A rotavirus, Ausjesky Disease Virus, and other herpesviruses) were investigated by molecular methods in the appropriate tissues. All samples tested negative. Although Eurasian badgers can be susceptible to several pathogenic bacteria (Wragg et al., 2011; Sin et al., 2014; Franzo et al., 2017; Judge et al., 2017), the isolates identified in this study probably represent contaminants, as histopathological analysis did not show any bacteria in the tissues or tissue alterations that could be related with the bacterial species isolated. *Micrococcus* and *Staphylococcus,* identified in badger B5 are common skin commensals of animals and humans, while *Clostridium* and *Escherichia coli*, belong to their intestinal microbiota (Quinn et al., 2011)). Also, to the best of our knowledge, the first three genera have not yet been related to bacterial infections in *Meles meles*, while *E. coli* was reported in badgers' bronchoalveolar lavages (McCarthy et al., 2009).

The viral loads found in the tested organs (Table 2), ranged from 1.19×10^3 to 2.99×10^6, despite kidney, heart and lungs tested negative in some badgers. These values were lower than the ones described for domestic and wild-rabbit (Carvalho et al., 2017), but are compatible with a systemic infection, following the possible ingestion of RHDV2 positive rabbits. However, the mere passage of the virus through the gastrointestinal tract, without surpassing this barrier, would result in faeces and intestine and, at most, the mesenteric lymph nodes testing positivity, while all the other organs would test negative. That was not the case since liver, lungs and spleen showed consistent and relatively high viral loads.

Amplification and sequencing analysis of a 2,188-nt long fragment comprising part of the RdRp gene and the complete the VP60 gene verified the presence of RHDV2-RNA in the tissues of badgers B5 and B6. For badgers B1, B7, B8 and B9 (as summarized in Table S1), only partial sequences of the RdRp gene were obtained, however also confirming the RT-qPCR results by demonstrating unequivocally the presence of viral RNA in the badgers' tissues.

The molecular data was supported by the immunohistochemistry, immunofluorescence, and dot blot results, alongside the gross pathology and histopathological lesions. Dot blot analysis of liver homogenates from badger B5 and B6, confirmed the presence of RHDV or RHDV2 protein in these organs. Curiously, the dot blot signal in B6 was stronger than in B5, despite the RT-qPCR results showed higher viral loads (deduced from the number of RNA copies) in B5 tissues. However, dot blot is not a quantitative technique and tissue homogenizations for dot blot were not carried out as accurately as for RNA extraction.

Gross pathology and histopathology suggest that multiorgan failure (heart, kidney and lung) could account for the proximal cause of death. The presence of iron deposits in the spleen, liver and lungs indicate haemorrhagic events, possibly due to chronic blood losses, more severe in the case of badgers B5 and B8, whose spleens were highly infiltrated with hemosiderin-laden macrophages. Although liver necrosis in badgers was not as evident as normally seen in rabbits infected with RHDV2 (Soliman et al., 2016; Abade dos Santos et al., 2017; Umer et al., 2017), hepatocytes showed hydropic degeneration and individual cell necrosis. Another difference from rabbits is the lymphoid hyperplasia that was observed in three of four analyzed badgers. This may indicate a more adjusted response to the viral infection, in accordance with the lower viral loads observed in the badgers, compared with rabbits.

Altogether, despite not so severe, the lesions observed may be accounted for a poor clinical evolution, leading to a moribund status incompatible with survival in the wild, taking into account that a weakened animal hardly survives, especially if in need to prey for food.

Additionally, the lower severity of the lesions compared to rabbits seems to indicate a less aggressive viral infection in this species. However, no studies are comparing the lesions caused by different GI.2 strains, namely by GI.4P/GI.2 strains. Despite different GI.2 strains showing different virulence were described, there is no data relating possible differences in the severity and type of lesions induced in rabbits with different strains. The pattern and severity of lesions may also change according to the clinical evolution, which in turn could vary due to intrinsic individual or species-related resistance and natural or acquired immunity to the infection. Nonetheless, If the course of the infection is less fulminating in badgers than in rabbits, probably because the badger is not a usual host of this virus, it may favor the dissemination of RHDV2 as a disease with a longer course will allow virus excretion in the faeces for longer.

Finally, by transmission electron microscopy we demonstrated the presence of viral particles compatible with RHDV2 in the badgers' tissues. Despite the poor preservation condition of the tissues, viral factories were observed providing evidence of active replication of the virus in the cells. Furthermore, the observation of viral factories in the hepatocyte nucleus revealed, we believe that for the first time, the RHDV2 passage through the nucleus during replication. This observation was previously reported in RHDV infected hepatocytes by Marcato et al. (Marcato et al., 1991). The meaning of this finding is still unclear, given that a nuclear phase was not described in the replicative cycle of Caliciviridae. Although the breakdown of the cell nuclear membrane may have allowed virions to pass into the nucleus as suggested before (Pesavento et al., 2004), since virions were exclusively grouped resembling viral factories, this scenario is unlikely. On the other hand, these clusters of virions within the nucleus were observed in several cells, where virions were not present in the cytoplasm of the same cells. The presence of virions compatible with RHDV2 has already been observed by our team in the nucleus of hepatocyte cells from rabbits that died infected with RHDV2 (*data not shown).* This may not be surprising since the presence of viral factories in the nucleus of infected cells was previously described in feline calicivirus infection (Pesavento et al., 2004).

By immunofluorescence, we confirmed the presence of many lysosomes or autophagosome structures in the hepatocyte cytoplasm, containing mature virions (Figure 15). As previously described (Vallejo et al., 2014), after RHDV infection, the host cells initiate a rapid autophagic response that declines, culminating in apoptosis. The vesicles shown in Figure 15, were also observed in RHDV infected liver cells by these same authors.

During the +Coelho project, a total of 25 dead rabbits from the Santarém district were sampled between March 2017 and March 2020, of which 15 (60%) were positive for RHDV2.

To the best of our knowledge, no lagoviruses had ever been described in wild badgers, in natural or experimental infections. In this study, we provide evidence that RHDV2 may have crossed another species barrier from the Leporidae family (order Lagomorpha) to the Mustelidae family (order Carnivora), a remarkable paradigm shift for the pathogenic potential of this virus.

More studies are now needed to understand if these cases represent a set of individual spillover events or a true species jump. The detection of RHDV2 in badgers along three consecutive years (2017-2020) supports, in our opinion, the second scenario, but further investigations are necessary to confirm the geographic extension of this event.

Another future interesting study concerns the research of other calicivirus in this species, namely viruses close to non-pathogenic lagoviruses, which may serve as donors of genetic material and thus contribute to the evolution of *Lagovirus europaeus* and the emergence of new pathogenic strains.

Experimental infections with European badgers would help to clarify the baseline level of susceptibility to infection, however, they are extremely complicated in protected species. Nonetheless, priority investigations should include RHDV2 monitoring in badgers in Santarém District and other geographical areas, monitoring viral evolution within this host species, evaluating the pathogenic impact of RHDV2 strains adapted to badgers towards rabbits and to understand the role of the Eurasian badger as a reservoir host for RHDV2.

Authors' contributions

Abade dos Santos, F.A.: Conceptualization, Investigation, Methodology, Resources, Writing – Original Draft Preparation

Pinto, A.: Formal analysis, Investigation, Methodology, Resources

Burgoyne, Thomas.: Investigation, Resources

Dalton, K.P.: Investigation, Resources, Validation

Carvalho C.L.: Investigation

Ramilo, D.: Investigation

Carneiro, C.: Investigation

Carvalho, T.: Investigation, Writing – Review & Editing

Peleteiro, M.C.: Funding Acquisition, Supervision, Visualization, Validation, Writing – Review & Editing

Parra, F.: Conceptualization, Funding acquisition, Supervision, Validation, Writing – Review & Editing

Duarte, M.D.: Conceptualization, Funding acquisition, Investigation, Project Administration, Supervision, Validation, Writing – Review & Editing

Ethical Statement

This study did not use live animals and was carried out within the scope of a National Plan (+Coelho2, Dispatch no. 4757/2017 of 31 May), with the legal authorizations from the National Authority-the Institute for Nature Conservation and Forests (Instituto da Conservação da Natureza e das Florestas, I.P., ICNF).

Conflict of interest

The authors declare no competing interests.

References

Abade dos Santos, F.A., C. Carvalho, O. Nuno, J.J. Correia, M. Henriques, M.C. Peleteiro, M. Fevereiro, and M.D. Duarte, 2017: Detection of rabbit Haemorrhagic disease virus 2 during the wild rabbit (Oryctolagus cuniculus) eradication from the Berlengas archipelago, Portugal. *BMC Vet. Res.* **13**, 336, DOI: 10.1186/s12917-017-1257-3.

Abrantes, J., C. Droillard, A.M. Lopes, E. Lemaitre, P. Lucas, Y. Blanchard, S. Marchandeau, P.J. Esteves, and G. Le Gall-Reculé, 2020: Recombination at the emergence of the pathogenic

rabbit haemorrhagic disease virus Lagovirus europaeus/GI.2. *Sci. Rep.* **10**, 1–12, DOI: 10.1038/s41598-020-71303-4.

Bancroft, J.D., and A. Stevens, 1982: Theory and Practice of Histological Techniques, 3rd edn. Edinburgh: Churchill Livingstone.

Calvete, C., M. Mendoza, M.. Sarto, M.P. Jiménez de Bagués, L. Luján, J. Molín, A.J. Calvo, F. Monroy, and J.H. Calvo, 2019: Detection of Rabbit Hemorrhagic Disease Virus GI . 2 / RHDV2 / B in the Mediterranean Pine Vole (Microtus duodecimcostatus) and White- Toothed Shrew (Crocidura russula). **55**, 1–6, DOI: 10.7589/2018-05-124.

Camarda, A., N. Pugliese, P. Cavadini, E. Circella, L. Capucci, A. Caroli, M. Legretto, E. Mallia, and A. Lavazza, 2014: Detection of the new emerging rabbit haemorrhagic disease type 2 virus (RHDV2) in Sicily from rabbit (Oryctolagus cuniculus) and Italian hare (Lepus corsicanus). *Res. Vet. Sci.* **97**, 642–645, DOI: 10.1016/j.rvsc.2014.10.008.

Capucci, L., P. Fusi, a Lavazza, M.L. Pacciarini, and C. Rossi, 1996: Detection and preliminary characterization of a new rabbit calicivirus related to rabbit hemorrhagic disease virus but nonpathogenic. *J. Virol.* **70**, 8614–8623.

Capucci, L., M. Scicluna, and A. Lavazza, 1991: Diagnosis of viral haemorrhagic disease of rabbits and the European brown hare syndrome. *Rev Sci Tech* **10**, 347–370.

Carvalho, C.L., E.L. Duarte, M. Monteiro, A. Botelho, T. Albuquerque, M. Fevereiro, A.M. Henriques, S.S. Barros, and M.D. Duarte, 2017: Challenges in the rabbit haemorrhagic disease 2 (RHDV2) molecular diagnosis of vaccinated rabbits. *Vet. Microbiol.* **198**, 43–50, DOI: 10.1016/j.vetmic.2016.12.006.

Chiari, M., S. Molinari, P. Cavadini, B. Bertasi, M. Zanoni, L. Capucci, and A. Lavazza, 2016: Red foxes (Vulpes vulpes) feeding brown hares (Lepus europaeus) infected by European brown hare syndrome virus (EBHSv) might be involved in the spread of the virus. *Eur. J. Wildl. Res.*761–765, DOI: 10.1007/s10344-016-1055-4.

Dalton, K.P., J.L. Arnal, A.A. Benito, G. Chacón, J.M. Martín Alonso, and F. Parra, 2018: Conventional and real time RT-PCR assays for the detection and differentiation of variant rabbit hemorrhagic disease virus (RHDVb) and its recombinants. *J. Virol. Methods* **251**, 118–122, DOI: 10.1016/j.jviromet.2017.10.009.

Di Profio, F., I. Melegari, V. Sarchese, and S. Robetto, 2017: Potential role of wolf (Canis lupus) as passive carrier of European brown hare syndrome virus (EBHSV) Research in Veterinary Science Potential role of wolf (Canis lupus) as passive carrier of European brown hare

syndrome virus (EBHSV). *Res. Vet. Sci.* **117**, 81–84, DOI: 10.1016/j.rvsc.2017.11.016.

Duarte, M.D., C.L. Carvalho, S.C. Barros, A.M. Henriques, F. Ramos, T. Fagulha, T. Luís, E.L. Duarte, and M. Fevereiro, 2015: A real time Taqman RT-PCR for the detection of rabbit hemorrhagic disease virus 2 (RHDV2). *J. Virol. Methods* **219**, 90–95, DOI: 10.1016/j.jviromet.2015.03.017.

Fedriani, J.M., F. Palomares, and M. Delibes, 1999: Niche relations among three sympatric Mediterranean carnivores. *Oecologia* **121**, 138–148, DOI: 10.1007/s004420050915.

Franzo, G., P. Massi, C.M. Tucciarone, I. Barbieri, G. Tosi, L. Fiorentini, M. Ciccozzi, A. Lavazza, M. Cecchinato, and A. Moreno, 2017: Think globally, act locally: Phylodynamic reconstruction of infectious bronchitis virus (IBV) QX genotype (GI-19 lineage) reveals different population dynamics and spreading patterns when evaluated on different epidemiological scales. *PLoS One* **12**, 1–20, DOI: 10.1371/journal.pone.0184401.

González, A.M., 2019: Caracterización antigénica y diseño de vacunas frente a la nueva variante del virus de la enfermedad hemorrágica del conejo. PhD thesis, University of Oviedo.

Judge, J., G.J. Wilson, R. Macarthur, R.A. McDonald, and R.J. Delahay, 2017: Abundance of badgers (Meles meles) in England and Wales. *Sci. Rep.* **7**, 1–8, DOI: 10.1038/s41598-017-00378-3.

Kumar, S., G. Stecher, M. Li, C. Knyaz, and K. Tamura, 2018: MEGA X: Molecular Evolutionary Genetics Analysis across computing platforms. Molecular Biology and Evolution. .

Le Gall-Recule, G., F. Zwingelstein, S. Boucher, B. Le Normand, G. Plassiart, Y. Portejoie, A. Decors, S. Bertagnoli, J.-L. Guerin, and S. Marchandeau, 2011: Detection of a new variant of rabbit haemorrhagic disease virus in France. *Vet. Rec.* **168**, 137–138, DOI: 10.1136/vr.d697.

Le Gall-Reculé, G., F. Zwingelstein, M.P. Fages, S. Bertagnoli, J. Gelfi, J. Aubineau, A. Roobrouck, G. Botti, A. Lavazza, and S. Marchandeau, 2011: Characterisation of a non-pathogenic and non-protective infectious rabbit lagovirus related to RHDV. *Virology* **410**, 395–402, DOI: 10.1016/j.virol.2010.12.001.

Le Pendu, J., J. Abrantes, S. Bertagnoli, J.-S. Guitton, G. Le Gall-Reculé, A.M. Lopes, S. Marchandeau, F. Alda, T. Almeida, A.P. Célio, J. Bárcena, G. Burmakina, E. Blanco, C. Calvete, P. Cavadini, B. Cooke, K. Dalton, M. Delibes Mateos, W. Deptula, J.S. Eden, F. Wang, C.C. Ferreira, P. Ferreira, P. Foronda, D. Gonçalves, D. Gavier-Widén, R. Hall, B. Hukowska-Szematowicz, P. Kerr, J. Kovaliski, A. Lavazza, J. Mahar, A. Malogolovkin, R.M. Marques, S. Marques, A. Martin-Alonso, P. Monterroso, S. Moreno, G. Mutze, A. Neimanis, P.

Niedzwiedzka-Rystwej, D. Peacock, F. Parra, M. Rocchi, C. Rouco, N. Ruvoën-Clouet, E. Silva, D. Silvério, T. Strive, G. Thompson, B. Tokarz-Deptula, and P. Esteves, 2017: Proposal for a unified classification system and nomenclature of lagoviruses. *J. Gen. Virol.* **98**, 1658—1666, DOI: 10.1099/jgv.0.000840.

Liu, S., H. Xue, B. Pu, and N. Qian, 1984: A new viral disease in rabbit. *Anim Husb Vet Med* **16**, 253–255.

Lopes, A.M., S. Marques, E. Silva, M.J. Magalhães, A. Pinheiro, P.C. Alves, J. Le Pendu, P.J. Esteves, G. Thompson, and J. Abrantes, 2014: Detection of RHDV strains in the Iberian hare (Lepus granatensis): Earliest evidence of rabbit lagovirus cross-species infection. *Vet. Res.* **45**, 1–7, DOI: 10.1186/s13567-014-0094-7.

Mahar, J.E., R.N. Hall, D. Peacock, J. Kovaliski, M. Piper, R. Mourant, and N. Huang, 2018: Rabbit Hemorrhagic Disease Virus 2 (RHDV2; GI.2) Is Replacing Endemic Strains of RHDV in the Australian Landscape within 18 Months of Its Arrival. *J. Virol.* **2**, 1–15, DOI: https://doi.org/10.1128/JVI.01374-17. Editor.

Marcato, P., C. Benazzi, G. Vecchi, M. Galeotti, L. Della Salda, G. Sarli, and P. Lucidi, 1991: Clinical and pathological features of viral haemorrhagic disease of rabbits and the European brown hare syndrome. *Rev Sci Tech* **10**, 371–392.

McCarthy, G., R. Shiel, L. O'Rourke, D. Murphy, L. Corner, E. Costello, and E. Gormley, 2009: Bronchoalveolar lavage cytology from captive badgers. *Vet. Clin. Pathol.* **38**, 381–387, DOI: 10.1111/j.1939-165X.2009.00127.x.

Meyers, G., C. Wirblich, and H.J. Thiel, 1991: Rabbit hemorrhagic disease virus-molecular cloning and nucleotide sequencing of a calicivirus genome. *Virology* **184**, 664–676, DOI: 10.1016/0042-6822(91)90436-F.

Mutze, G., P. Bird, J. Kovaliski, D. Peacock, S. Jennings, and B. Cooke, 2002: Emerging epidemiological patterns in rabbit haemorrhagic disease, its interaction with myxomatosis, and their effects on rabbit populations in South Australia. *Wildl. Res.* **29**, 577–590, DOI: 10.1071/WR00100.

Nei, M., and S. Kumar, 2000: Molecular Evolution and Phylogenetics. New York: Oxford University Press.

Neimanis, A.S., H. Ahola, U.L. Pettersson, A.M. Lopes, J. Abrantes, S. Zohari, P.J. Esteves, and D. Gavier-widén, 2018: Overcoming species barriers : an outbreak of Lagovirus europaeus GI . 2 / RHDV2 in an isolated population of mountain hares (Lepus timidus). 1–12.

Ohlinger, V.F., B. Haas, G. Meyers, F. Weiland, and H.-J. Thiel, 1990: Identification and Characterization of the Virus Causing Rabbit Hemorrhagic Disease. *J. Virol.* **64**, 3331–3336.

OIE, 2019: Rabbit haemorrhagic disease (Technical disease card). 1–7. OIE.

Peleteiro, M.C., J. Ferreira da Silva, P. Dias-Pereira, T. Carvalho, A. Faustino, J. Correia, H. Pissarra, and G. Stilwell, 2016: Manual de Necrópsia Veterinária1ª. (Lidel, Ed.). Lisbao.

Pesavento, P.A., N.J. Maclachlan, L. Dillard-Telm, C.K. Grant, and K.F. Hurley, 2004: Pathologic, immunohistochemical, and electron microscopic findings in naturally occurring virulent systemic feline calicivirus infection in cats. *Vet. Pathol.* **41**, 257–263, DOI: 10.1354/vp.41-3-257.

Puggioni, G., P. Cavadini, C. Maestrale, R. Scivoli, G. Botti, C. Ligios, G. Le Gall-Reculé, A. Lavazza, and L. Capucci, 2013: The new French 2010 Rabbit Hemorrhagic Disease Virus causes an RHD-like disease in the Sardinian Cape hare (Lepus capensis mediterraneus). *Vet. Res.* **44**, 1–7, DOI: 10.1186/1297-9716-44-96.

Quinn, P., B. Markey, F. Leonard, P. Hartigan, S. Fanning, and E. Fitzpatrick, 2011: Animal Diversity, Natural History and Conservation – Volume 22nd Editio., pp. 1–17. In: Rosalino, LM, T Sales-Luis, M Pinto Basto, NM Pedroso, L Tavares, CL Vilela, and M. Oliveira (eds), Veterinary Microbiology and Microbial Disease. Wiley-Blackwell.

Silvério, D., A.M. Lopes, J. Melo-ferreira, M.J. Magalhaes, P. Ponterroso, A. Serronha, E. Maio, P.C. Alves, P.J. Esteves, and J. Abrantes, 2018: Insights into the evolution of the new variant rabbit haemorrhagic disease virus (GI . 2) and the identification of novel recombinant strains. *Transbound. Emerg. Dis.* **00**, 1–10, DOI: 10.1111/tbed.12830.

Sin, Y.W., G. Annavi, H.L. Dugdale, C. Newman, T. Burke, and D.W. MacDonald, 2014: Pathogen burden, co-infection and major histocompatibility complex variability in the European badger (Meles meles). *Mol. Ecol.* **23**, 5072–5088, DOI: 10.1111/mec.12917.

Soliman, M., M. Rhaman, M. Samy, O. Mehana, and S. Nasef, 2016: Molecular, Clinical and Pathological Studies on Viral Rabbit Hemorrhagic Disease. *Alexandria J. Vet. Sci.* **48**, 20, DOI: 10.5455/ajvs.207505.

Strive, T., J.D. Wright, and A.J. Robinson, 2009: Identification and partial characterisation of a new lagovirus in Australian wild rabbits. *Virology* **384**, 97–105, DOI: 10.1016/j.virol.2008.11.004.

Umer, F., W.U. Riasat, L. Asma, B.Z. Aamer, I.D. Javid, and I. Hamid, 2017: Gross Pathological Findings of Rabbit Hemorrhagic Disease (RHD) in Two (02) Cases Case Report Gross Pathological Findings of Rabbit Hemorrhagic Disease (RHD) in Two. *Res. J. Vet. Pract.* **1 (4)**, 39–40.

USDA, 2020: Emerging Risk Notice. Rabbit Hemorrhagic Disease Virus, Type 2. .

Vallejo, D., I. Crespo, B. San-Miguel, M. Álvarez, J. Prieto, M.J. Tuñón, and J. González-Gallego, 2014: Autophagic response in the Rabbit Hemorrhagic Disease, an animal model of virally-induced fulminant hepatic failure. *Vet. Res.* **45**, 1–13, DOI: 10.1186/1297-9716-45-15.

Velarde, R., P. Cavadini, A. Neimanis, O. Cabezón, M. Chiari, A. Gaffuri, S. Lavín, G. Grilli, D. Gavier-Widén, A. Lavazza, and L. Capucci, 2017: Spillover Events of Infection of Brown Hares (Lepus europaeus) with Rabbit Haemorrhagic Disease Type 2 Virus (RHDV2) Caused Sporadic Cases of an European Brown Hare Syndrome-Like Disease in Italy and Spain. *Transbound. Emerg. Dis.* **64**, 1750–1761, DOI: 10.1111/tbed.12562.

Wragg, P.N., B.W. Strugnell, A.M. Whatmore, and G. Foster, 2011: Arcanobacterium haemolyticum in a badger (Meles meles). *J. Vet. Diagnostic Investig.* **23**, 1234–1235, DOI: 10.1177/1040638711425585.